

Study of a Threshold Cherenkov Counter Based on Silica Aerogels with Low Refractive Indices *

I. Adachi[†], T. Sumiyoshi, K. Hayashi, N. Iida, R. Enomoto, K. Tsukada
National Laboratory for High Energy Physics(KEK), 1-1 Oho, Tsukuba, Ibaraki 305, Japan

R. Suda, S. Matsumoto, K. Natori
Department of Physics, Chuo University, 1-13-27 Kasuga, Bunkyo-ku, Tokyo 112, Japan

M. Yokoyama, H. Yokogawa
Central Research Laboratory, Matsushita Electric Works, Ltd., 1048 Kadoma, Osaka 571, Japan

Abstract

To identify π^\pm and K^\pm in the region of $1.0 \sim 2.5$ GeV/c, a threshold Cherenkov counter equipped with silica aerogels has been investigated. Silica aerogels with a low refractive index of 1.013 have been successfully produced using a new technique. By making use of these aerogels as radiators, we have constructed a Cherenkov counter and have checked its properties in a test beam. The obtained results have demonstrated that our aerogel was transparent enough to make up for loss of the Cherenkov photon yield due to a low refractive index. Various configurations for the photon collection system and some types of photomultipliers, such as the fine-mesh type, for a read out were also tested. From these studies, our design of a Cherenkov counter dedicated to π/K separation up to a few GeV/c with an efficiency greater than 90 % was considered.

1 Introduction

Recently, asymmetric e^+e^- colliders with high luminosities to explore CP violation in B meson system (B -factory) have been proposed[1, 2]. In a B -factory detector, an identification of the particle species is an important issue. In particular, the separation of π^\pm and K^\pm in the momentum region of $1.0 \sim 2.5$ GeV/c is indispensable for studying many B meson decay channels[1]. For this purpose, Cherenkov counter equipped with silica aerogels having a low refractive index is one of the most promising devices since it has been widely used in high energy experiments[3]. Furthermore, the use of an aerogel Cherenkov counter enables us to reduce the material for a particle identification device which is located in front of an electromagnetic calorimeter.

The requirements imposed on our aerogel Cherenkov counter are: (i) The refractive index of aerogel (n) should be in the $1.010 \sim 1.015$ range in order to achieve a π/K separation capability in the region of $1.0 \sim 2.5$ GeV/c. (ii) The optical transparency of the aerogel should be high. Notice that Cherenkov photons emitted by an injected particle becomes significantly small in our case because the Cherenkov light yields are proportional to $1 - 1/n^2$. Therefore, the loss of photons in the aerogel due to absorptions and scatterings should be minimized. (iii) Efficient photon collection and detection under a

*to be published in Nucl. Instrum. Meth. **A**

[†] internet address: ichirou@kekvox.kek.jp

strong magnetic field in the counter have to be considered to avoid any inefficiency for π identification. We require that the detection efficiency of π identification should be greater than 90 %, thus resulting in the averaged number of photoelectrons greater than 2.5 for $\beta = 1$.

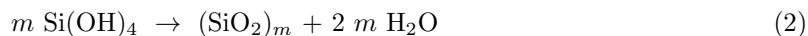
Because aerogels with $n < 1.02$ are not commercially available, we have developed a new aerogel production technique with low densities and high transparencies, and a test counter based on these aerogels has been built. Using this counter, the optical characteristics of aerogels and various conditions of counters were tested in order to optimize some parameters for our detector design.

In the next section, the production technique of our new aerogel is described. Their optical properties are given in section 3. Section 4 is devoted to results using a test beam. After describing basic properties of the new aerogels, an investigation of the light collection system, including tests of photomultipliers, is also given here. Based on the results from the beam test, a detector consideration is discussed in section 5. Finally, section 6 summarizes this paper.

2 Preparation of Aerogels

2.1 Single- and Two-Step Methods

Silica aerogel with a higher refractive index than 1.02 has been produced in a conventional single-step method[4, 5, 6, 7]. In this method, tetraalkoxysilane and water are mixed in an excess of alcohol as a solvent. The following hydrolysis and condensation of silicon alkoxides with the help of a catalyst are simultaneously proceeded in a single container:



In these two successive reactions, the solution becomes colloidal. Then, aging is done in order to form three-dimensional networks of SiO_2 clusters connected by a siloxan linkage. After the alcogel is made, it is dried in an autoclave at a point safely higher than the critical point(supercritical drying) to remove any alcohols. The density and, consequently the refractive index of the aerogel is mainly determined from the quantity of alcohol added in the first stage as a solvent. If the quantity of alcohol is increased in order to make low density aerogel, it becomes difficult to form a gel with high porosity since the backward reactions take place. This is why aerogels with low refractive indices or optically good properties can not be made using this method.

To make aerogel with a lower refractive index, a “two-step sol-gel” method has been developed at Lawrence Livermore National Laboratory[8]. They produce partially hydrolysed and partially condensed silica oil in the first step. Next, the alcohol is distilled off from the silica oil. This solution is called a “precursor”. Then, it is mixed with a non-alcohol solvent, and polymerization is then performed by adding an alkali catalyst, which makes SiO_2 cluster pores having a smaller size than an acid catalyst does. The gels, after aging, were dried under the supercritical condition, yielding a high-porosity aerogel with a low refractive index. This two-step method is one of the best ways to produce aerogels having a low refractive index. There are, however, some complicated processes, such as the distillation of alcohol.

2.2 New Production Method

Our new production method of aerogels with a low refractive index is essentially the same as the single-step method except for the use of methylalkoxide “oligomer” instead of tetraalkoxysilane. Figs. 1 -(a) and -(b) are charts for the oligomer and the presursor in the two-step method obtained by a gas chromatograph mass-spectrometer, respectively. From these charts, we can compare compositions of the oligomer with

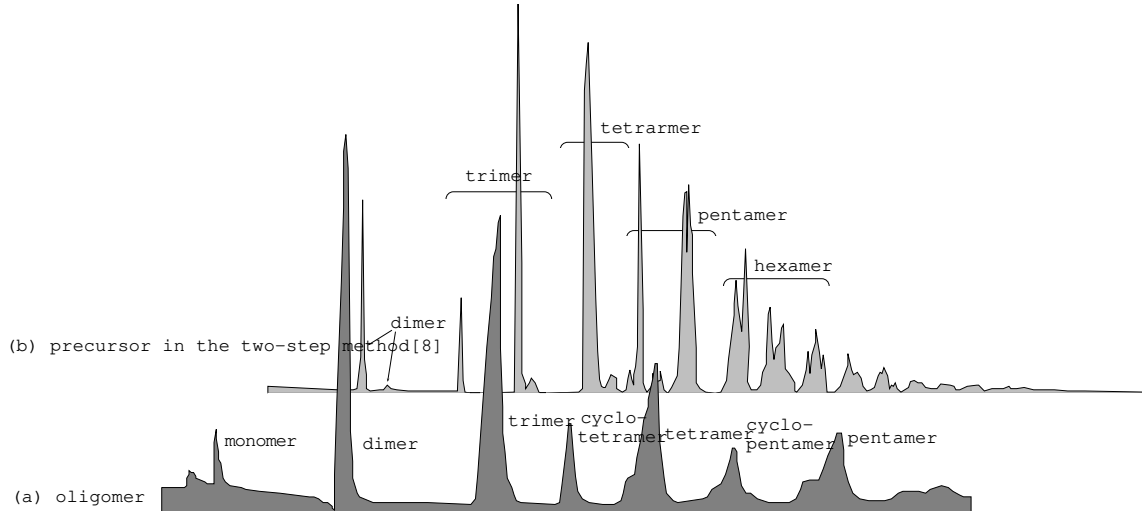


Fig.1

Figure 1: Charts for the oligomer(a) and the precursor(b) measured by the gas chromatograph mass-spectrometer. The horizontal and vertical directions correspond to the response time and the content of each composition, respectively.

those of the precursor. As can be seen, the compositions of the oligomer are almost identical to those of the precursor. Namely, the oligomer is a stable liquid after partial hydrolysatation and partial condensation. Therefore, the advantage of our method is to simplify the production processes, which is very important for the mass-production of aerogels, with keeping the merits of the two-step method. In addition, the oligomer can be easily obtained on a commercial basis and is not expensive.

Another advantage of our technique is the hydrophobic characteristic of the aerogels. In the production process, the characteristic of the alcogel can be changed so as to be hydrophobic by replacing any silanol groups(-OH) into hydrophobic ones.

Our production methods are as follows. At first, two solutions are prepared. One is made by adding an oligomer in ethyl alcohol as a solvent, and the other is distilled water with ethyl alcohol. Here, ammonia water is also added in this solution as an alkali catalyst to polymerize small and uniform pores. These two solutions are mixed in a polystyrene container at room temperature. After a few minutes, the gelation takes place, and the alcogel is made. The alcogel is put into a sealed vessel in order to suppress evaporation of the ethyl alcohol, and is kept at room temperature for one week. Then, the sealed vessel, in which the alcogel has been placed, is filled with ethyl alcohol vapor in order to proceed the formation of a three-dimensional network of SiO₂. After that, alcogel is moved into a stainless-steel bag from a polystyrene container and is left in ethyl alcohol for one week.

To make alcogel hydrophobic, special treatment is taken. The silanol groups on the surface of SiO₂ is likely to be charged and contacting other ions. It is thus replaced into Si(CH₃)₃ groups by adding hydrophobic agent, for example, hexamethyldisilazane, into ethyl alcohol, as shown in Fig. 2. This solution, in which the alcogel is moved, is stirred by an electrical power agitator at 40 ~ 60°. This process is completed in 3 ~ 24 hours, which depends on the temperature. The replacement of the hydrophilic groups in the alcogel with hydrophobic ones also plays an important role in preserving its

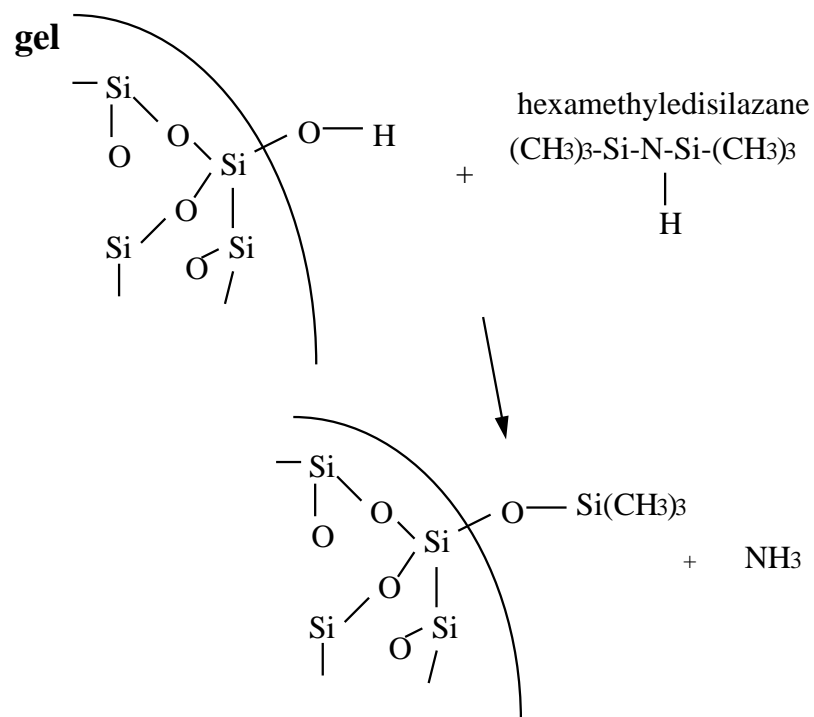


Fig. 2

Figure 2: Schematic drawing of the hydrophobic reaction of the alcogel.

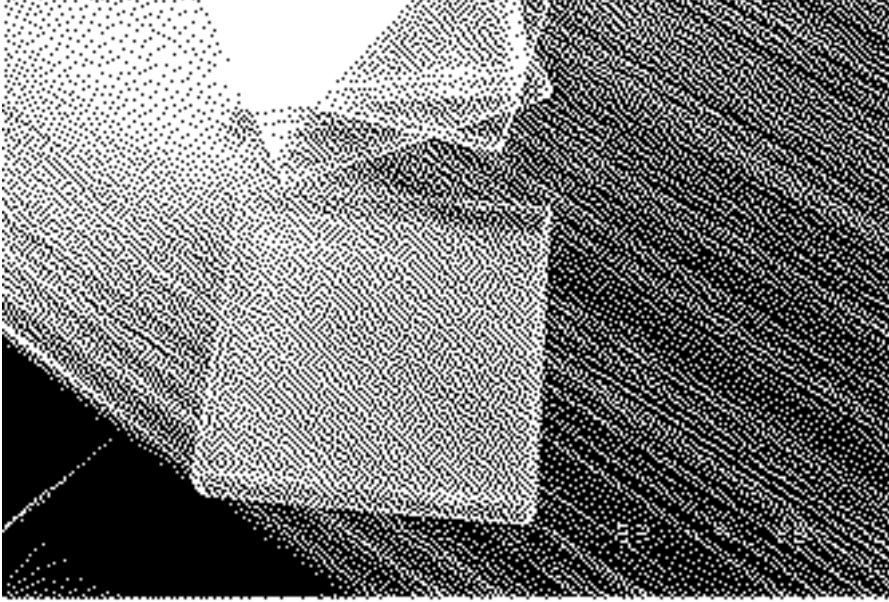


Figure 3: Photograph of the aerogel produced using the new technique.

volume after supercritical drying in an autoclave since shrinkage of the aerogel is considered to be due to the electrically attractive force among the silanol groups and/or between the silanol groups and other ions.

After this reaction, the alcogel is again sunk in ethyl alcohol, and the alcohol is replaced once every 3 days. During this period, ammonia in the alcogel, which was generated in the hydrophobic reaction, is solved into alcohol.

To transform the alcogel into aerogel, the alcogel is dried at the supercritical point. Here, alcohol is replaced into carbon dioxide before heating. The pressure and temperature at the supercritical point of carbon dioxide is much lower than that of ethyl alcohol. It, therefore, provides a safer and more economical benefits. A complete description can be found in Ref.[9]

An aerogel of 16×16 (cross section) \times 2(thick) cm^3 with $n = 1.013$ has been successfully made using this method. We produced 22 pieces of aerogels with this size. Fig. 3 is a photograph of the obtained aerogel. It was shrunk to be about 20 % in volume. Some cracks could be seen inside the volume or on its surface although they were tolerable. Its optical properties were described in the next section.

3 Optical Properties of New Aerogels

3.1 Transmission

The transmission of the aerogel obtained with the new method described above was measured using a photospectrometer[10]. The thickness of the aerogel of the sample was 2.2 cm. The obtained data can be translated into the transmission length(Λ) by the function:

$$T = T_0 \exp(-d/\Lambda), \quad (3)$$

where T and d are the transmission and thickness of the aerogel, respectively. Fig. 4 shows the transmission length as a function of the wave length(λ). The transmission length strongly depends on the wave

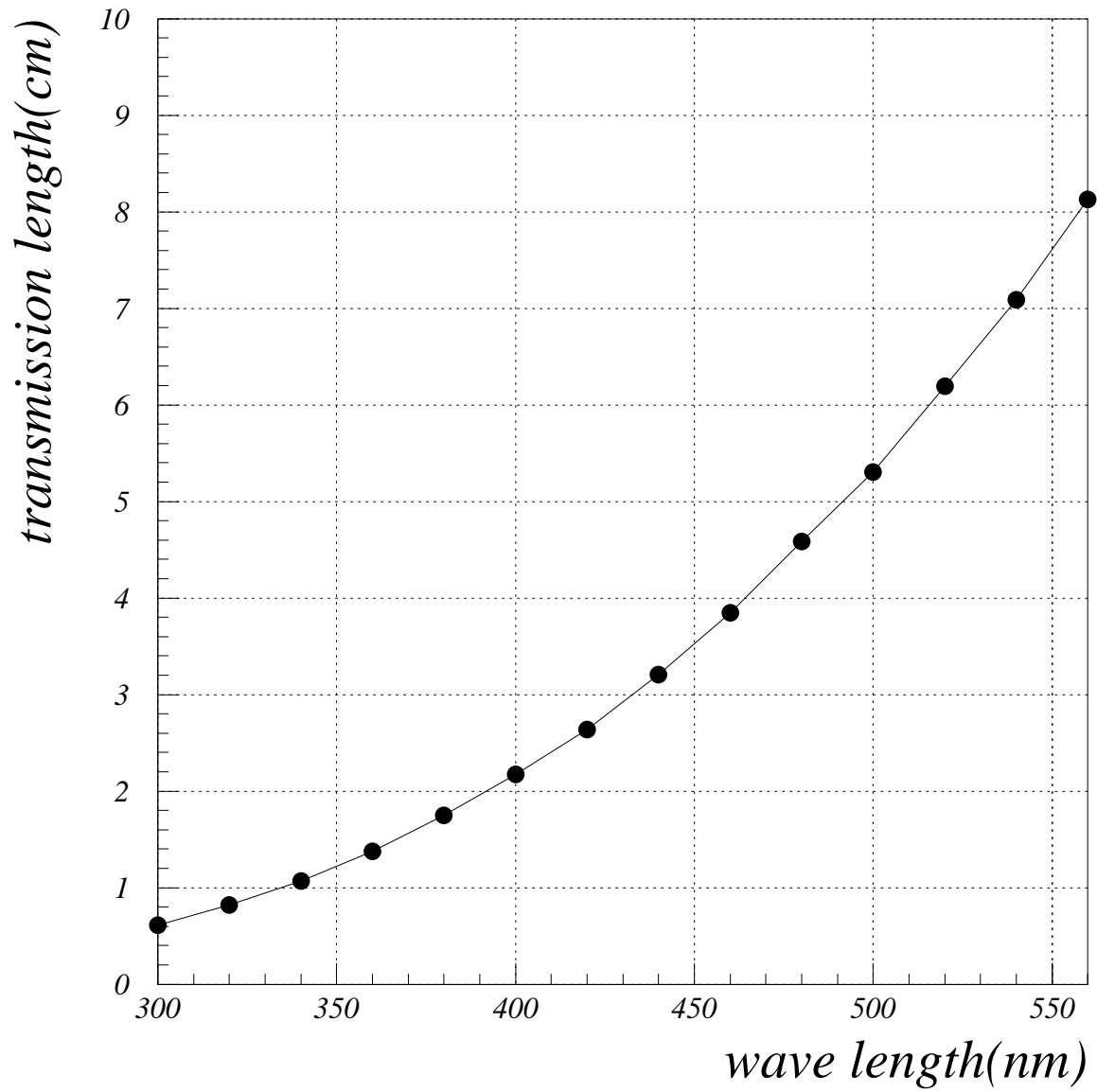


Figure 4: Transmission length(cm) as a function of the wave length(nm) obtained with a photospectrometer. The aerogel thickness is 2.2 cm.

wave length (nm)	this experiment $n = 1.013$	Ref.[4] $n = 1.024$	Ref.[5] $n = 1.058$	Ref.[6] $n = 1.058$	Ref.[7] $n = 1.055$
400	2.2		1.5	1.38	1.15
440	3.2	2.64	2.0		

Table 1: Summary of measurements of the transmission length(cm).

length. These effects can be related to the size and uniformity of microscopic pores of the aerogel. Our results are compared with those of other measurements in Table 1. Typically, the transmission length was obtained to be more than 3.0 cm at $\lambda = 440$ nm. Compared with aerogels used in high energy experiments so far, our aerogel is one of the most transparent ones.

3.2 Refractive Index

The refractive indices were determined using an optical method with a He-Ne laser beam of $\lambda = 632.8$ nm before the beam test. The minimum deflection of the incident laser beam after transversing one corner of the aerogel, which was placed on a movable table, was measured. This measurement was made for all of the aerogels produced. Most of them had refractive indices of 1.013, suggesting uniformity of the optical quality of the material.

4 Results of Beam Test

4.1 Experimental Set-up

This test was carried out at the $\pi 2$ beam line in KEK 12-GeV/c PS. The experimental layout is shown in Fig. 5. Negatively charged particles, mainly π^- , in the momentum range of $0.6 \sim 4.0$ GeV/c were used. The contribution from K^- was sufficiently small so as to be neglected over this momentum region. Although the fraction of electrons was small at 4.0 GeV/c, it increased with lower momentum and was sizeable below 1.0 GeV/c.

A test counter was located inside a tight black box for light shield. Two gas Cherenkov counters($C1$ and $C2$) were used to remove electrons from the pion beam. Three scintillation counters($S1 \sim S3$) and one anti-counter(AC) were placed upstream of the test counter, and one scintillation counter($S4$) was located downstream. $S1$ and $S2$ have cross sections of 5×5 cm² and 2×2 cm², respectively. The beam was defined to be 1×1 cm² by the $S3$ counter. AC was placed in front of the test counter to make sure that only one charged particle hits the test counter. The beam direction was definitely guaranteed by the $S4$ counter. A trigger was generated by the 3-fold coincidence of $S1 \sim S3$.

Analog signals from the test counter, together with all other counters, were fed into an ADC Lecroy 2249W, which was driven via a CAMAC system controlled from a personal computer.

In the off-line analysis, events which left reasonable signals in all of $S1 \sim S4$ counters and simultaneously no signals in AC were used. The electron contamination was also rejected by the $C1$ and $C2$ informations.

4.2 Test Counter Configuration

Fig. 6 shows a schematic drawing of the test Cherenkov counter. The test Cherenkov counter has a size of 16×16 cm² cross section and 25 cm height, where the active aerogel volume is $16 \times 16 \times 14$ cm³. Two holes with 2'' diameters were made in the side walls of the box to place photomultipliers(PMT's).

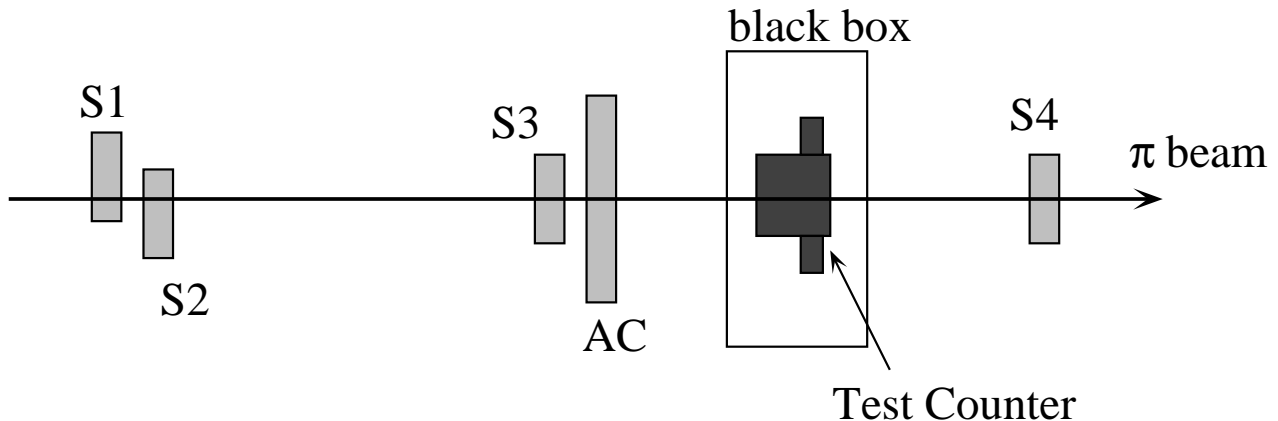


Fig.5

Figure 5: Schematic drawing of the experimental set-up.

Aerogel sheets were stacked in the box, and 2" PMT's were equipped in the holes for read out as indicated in Fig. 6. The internal surface was covered with white reflectors of Millipore sheets(GVHP00010).

To check the optical characteristics of the aerogels, 2" quantacon-type PMT (R3241 provided by Hamamatsu P.K.K.), which is able to detect a single photoelectron, was used. The high voltages applied to two PMT's were determined so that two gains were identical. This adjustment was carried out with a stable LED light source, of which the intensity was reduced to be equivalent to a single photon.

4.3 Evaluation of the Average Number of Photoelectrons

Figs. 7 -(a) and -(b) show the pulse height spectrum obtained by summing two 2" PMT's for 4 GeV/c and 1.5 GeV/c π^- , respectively. We extracted an average number of photoelectrons(N_{pe}) from these distributions. Some methods have been adopted to determine N_{pe} .

One method is to calculate the inefficiency from the number of pedestal events(N_{ped}). Assuming a Poissonian distribution, one can determine N_{pe} as:

$$N_{pe} = -\log(N_{ped}/N_{all}), \quad (4)$$

where N_{all} is the total number of events. In this method, N_{pe} can be evaluated without ambiguity when N_{pe} is less than 5. If N_{pe} becomes more than 5, we can not easily separate N_{ped} from the over-all pulse height distribution.

Another method is to fit the distribution by the function of the convolution of the Gaussian and Poissonian distributions expressed by:

$$f(x) = C \sum_{k=1}^{k_0} \frac{(N_{pe})^k e^{-N_{pe}}}{k!} \cdot \frac{1}{\sigma\sqrt{2\pi k}} \exp\left(\frac{-(x - pk)^2}{2k\sigma^2}\right), \quad (5)$$

where p corresponds to the interval between zero and single photoelectron peaks. σ is the standard deviation of a single photoelectron peak, and x is ADC channel after pedestal subtraction. C is a

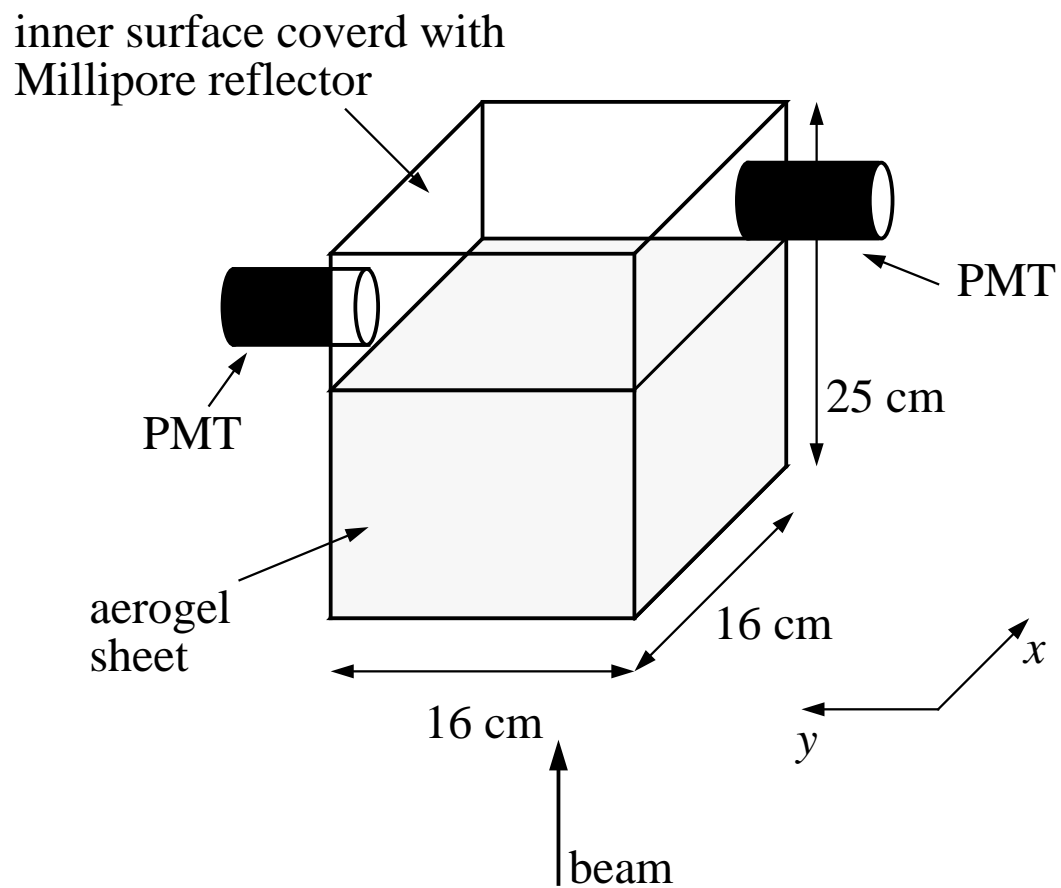


Fig.6

Figure 6: Schematic view of the test Cherenkov counter. The x - and y -axes were also indicated. The origin $(x, y) = (0, 0)$ was defined to be the center of the counter.

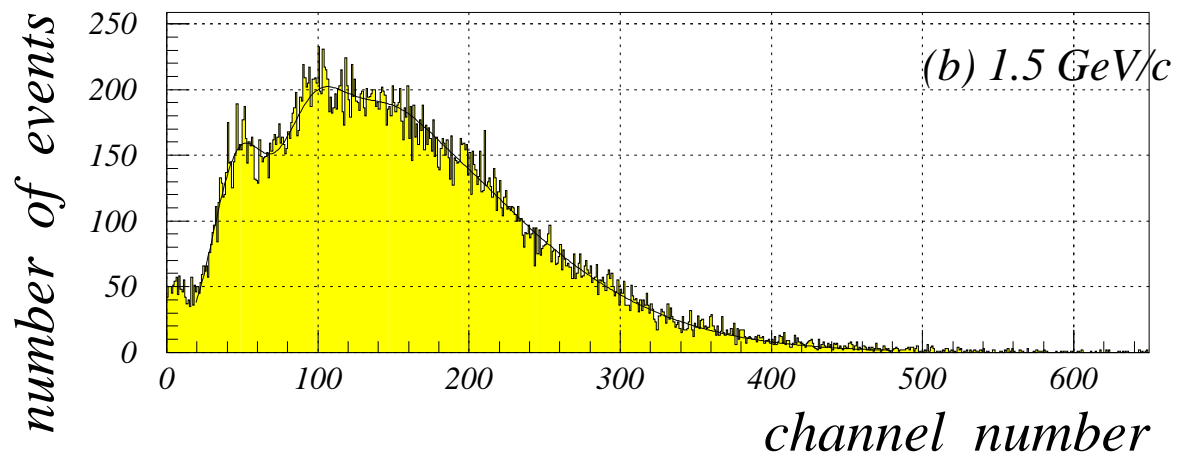
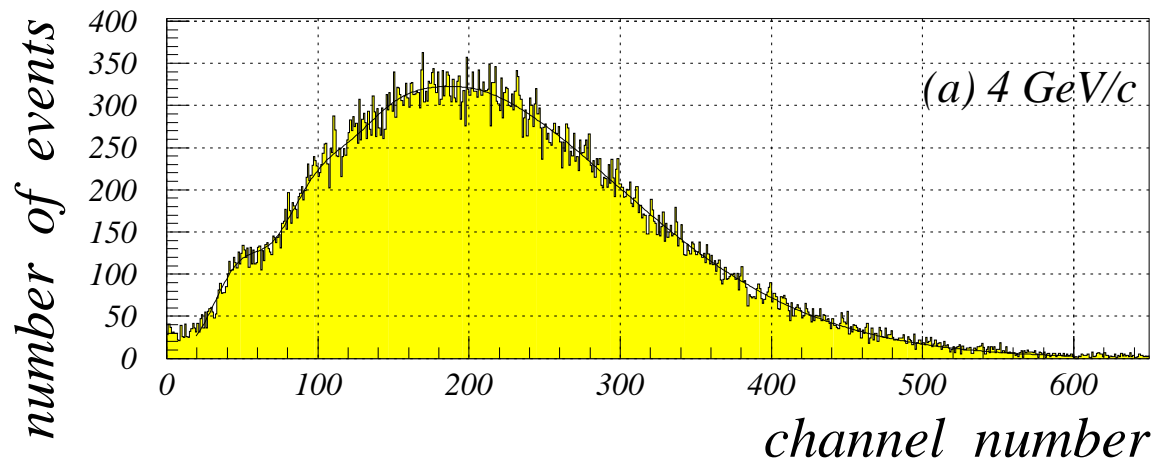


Figure 7: Pulse height distribution obtained by summing two 2'' quantacon-type PMT's for (a) 4 GeV/c and (b) 1.5 GeV/c π beam. The hatched histograms indicate the obtained data, whereas the solid curve is the best fit.

normalization constant. k_0 is the maximum number of photoelectron peaks contained in the distribution. This function assumed that the k -th photoelectron peak has a standard deviation of $\sqrt{k}\sigma$ and that the interval of photoelectrons is the same. In the fitting procedure, 4 parameters(N_{pe} , σ , p and C) were allowed to be free, whereas k_0 was fixed to be 10 so that the function of eq.5 could well reproduce the whole shape of the distribution.

In this analysis, the second method was employed unless specified. As a cross check, the first method was also used for several measurements, and the results from the two methods agreed well.

4.4 Thickness

The first check was made in order to determine the aerogel thickness to be used as a radiator. The thickness was varied by installing an additional wall, of which both sides were covered with Millipore sheets, between aerogel sheets so that the distance between the surface of the aerogel and the PMT was maintained. The beam was injected at the center of the test counter. Figs. 8 -(a) and -(b) show N_{pe} as functions of the thickness for 1.5 GeV/c and 4 GeV/c π^- , respectively. These behaviors can be well parametrized by:

$$N_{pe} = N_{max}(1 - \exp(-d/L)), \quad (6)$$

where d is the thickness, and L stands for the effective absorption length. L was obtained to be 4.23 ± 0.01 cm and 3.92 ± 0.04 cm for 4.0 GeV/c and 1.5 GeV/c, respectively. N_{max} is 4.23 ± 0.03 for 4.0 GeV/c π^- . The best-fit curves are also shown in the figures. The fitted curves well follow the obtained data. The photoelectron yield saturates at $d \sim 12$ cm, and 94.2 % of the photoelectrons can be detected at $d = 12$ cm.

In addition, we placed one more aerogel sheet into the counter, resulting in a thickness of 14 cm. However, the distance between the surface of the aerogel and the PMT's becomes smaller. The measured N_{pe} was increased to be 4.57 ± 0.01 by this configuration. This value is quite satisfactory. Though the Cherenkov photon yield significantly decreases as $1 - 1/n^2$ because of the low refractive index, we can compensate for this loss by producing highly transparent aerogels.

In what follows, we used this set-up having 14 cm aerogel sheets as a reference configuration.

4.5 Threshold Behavior

To measure the refractive indices of aerogels, the photoelectron yield was obtained by changing the momentum of the incident π^- particle which was injected at the center of the aerogel area. N_{pe} as a function of the inverse-square momentum of the incident particles is plotted in Fig. 9. In this analysis, N_{pe} was deduced from the pedestal events(eq. 4) in the region where the photoelectron yield was less than 1, since only pedestal peak can be seen in the obtained pulse height distribution and thus it is difficult to fit the function of the form of eq. 5. The momentum dependence of N_{pe} can be given by:

$$N_{pe} = C(1 - \frac{1}{n^2}(1 + \frac{m^2}{p^2})), \quad (7)$$

where n is the refractive index of aerogel, and m and p denote the mass and momentum of the incident particle, respectively. C is a constant which corresponds to the number of photoelectrons obtained at $\beta = 1$. The refractive index was estimated to be 1.0127 ± 0.0001 by fitting the obtained data above the threshold. Therefore, the threshold momentum was obtained to be 0.863 GeV/c and 3.05 GeV/c for π^\pm and K^\pm , respectively. This value was quite consistent with that from the optical measurement described previously.

It is important to estimate the knock-on effect because this effect produces a signal even for an incident particle with momentum below the threshold, causing a miss-identification of K as π . The knock-on effect can be estimated to be 10 % from the photoelectron value below the threshold momentum. This value is comparable with that obtained by other measurements[4].

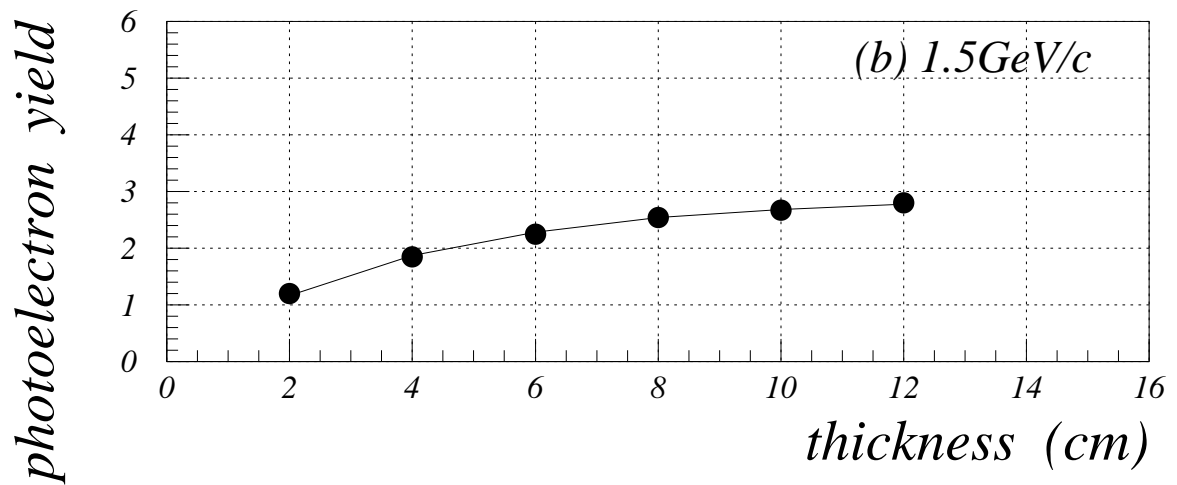
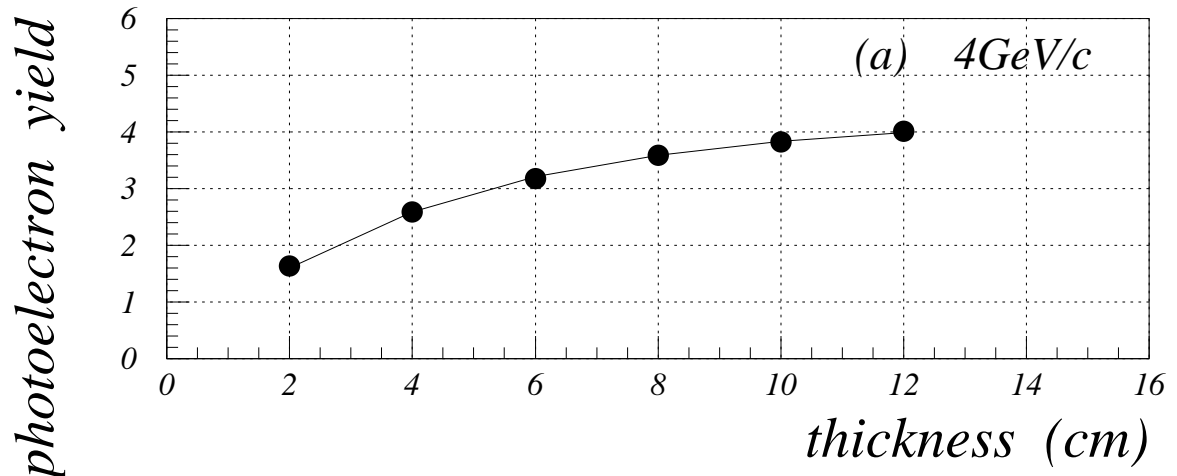


Figure 8: Average number of photoelectrons as functions of the aerogel thickness for (a) 4 GeV/c and (b) 1.5 GeV/c π beam. The measured data are plotted as closed circles, and the solid curves show the best-fitted function.

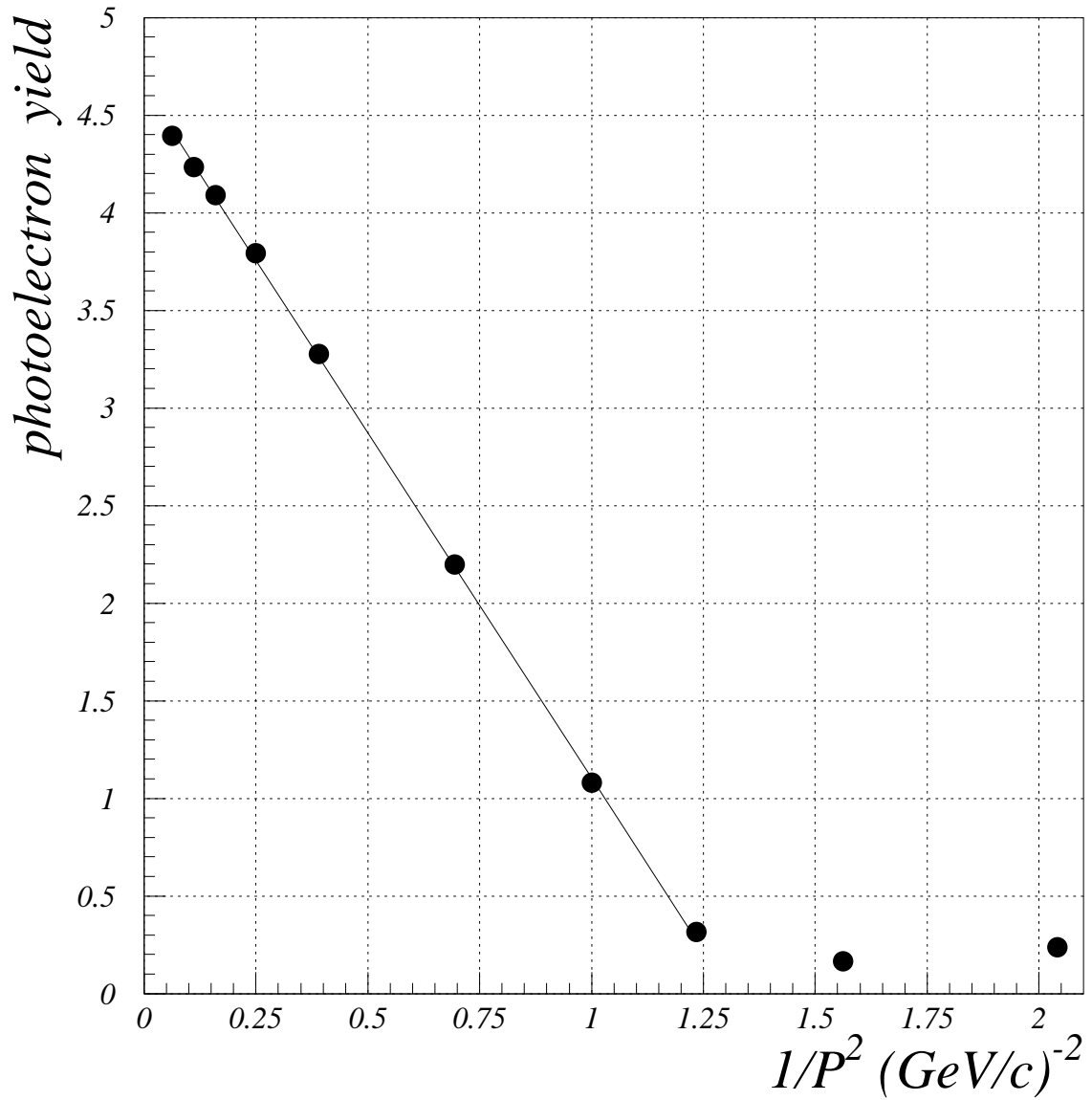


Figure 9: Average photoelectron yields as a function of the inverse momentum squared ($(\text{GeV}/c)^{-2}$). The closed circle is the obtained data, and the straight line is a fit to the data. The refractive index was obtained to be $n = 1.0127 \pm 0.0001$ from this fit.

momentum (GeV/c)	reference config.		type A	type B
	quantacon-type	fine-mesh	quantacon-type	quantacon-type
1.5	3.18 ± 0.01	1.95 ± 0.05	3.53 ± 0.01	3.96 ± 0.13
4.0	4.57 ± 0.01	2.74 ± 0.08	4.70 ± 0.01	4.77 ± 0.17

Table 2: Average number of photoelectrons obtained from various configurations. The types of the 2'' photomultipliers used are also listed. π^- was injected at the center of the aerogel.

4.6 Tests of The Counter Configuration

Some configurations for Cherenkov photon collection were tested. Basically, there are two kinds of photon collection systems.

One is a diffuse scattering technique, in which Cherenkov photons undergo scattering at the walls, which are covered with a highly efficient reflector, and reach the window of the PMT's. Accordingly, the directed photons as well as the scattered photons have a chance of being detected. We used this system as a reference configuration(as described before). Here, our interest is in the position dependence of the PMT's. Thus, the positions of the read out PMT's were changed as sketched in Fig. 10-(a) (type A).

Another type is to use a mirror to collect Cherenkov photons. This method collects only directed photons, which are determined by mirror optics. This type was also tested by installing a flat mirror as shown in Fig. 10-(b) (type B). The mirror was made of thin aluminum evaporated onto the fused glass. The surface of the aluminum was coated with MgF_2 .

In the case of center injection at 4.0 and 1.5 GeV/c π^- , the results for N_{pe} are listed in Table 2.

The position dependence of the incident particle was measured for three counter configurations; basic configuration(for a reference), type A and type B. The beam used was 4.0 GeV/c π^- . The x and y directions were defined as indicated in Fig. 10. Fig. reffig11 shows N_{pe} as a function of y at different x for the reference configuration. After summing pulse heights of two PMT's, the resultant N_{pe} has almost uniform response. The same figure, but for type A, is shown in Fig. 12. The same tendency can be seen. The results for type B are shown in Fig. 13. Although the mirror option provides the largest N_{pe} , it causes a strong dependence of the beam position.

From this study, it was found that type A gives better results than those from the reference configuration at the center injection and that for the uniform position dependence, on the other hand, type B provides maximum N_{pe} , but has a strong dependence on the beam position. Therefore, type A will be adopted for our final design.

4.7 Tests of Photomultipliers

In a realistic environment, a read out for an aerogel Cherenkov counter should be done in a strong magnetic field of 1 tesla. For this purpose, a fine-mesh type photomultiplier has been developed. To check the feasibility for aerogel read out with fine-mesh PMT's, two 2'' quantacon-type PMT's were replaced into two 2'' fine-mesh PMT's(R2490-05, assembly type, H2611 manufactured by Hamamatsu P.K.K.). This PMT contains 16 dynodes in the amplification stage. The gains of two PMT's were adjusted in the same way as mentioned previously. Here, a reference counter configuration was used, and 4.0 GeV/c and 1.5 GeV/c π beams were injected. Fig. 14 indicates the pulse height distribution detected from one fine-mesh PMT. No peak, but a long exponential-like tail, was observed. This phenomena is described in Ref.[11]. N_{pe} was extracted by counting the number of pedestal events. However, there was an ambiguity in separating pedestal events from the signal distribution. This uncertainty was estimated by varying the threshold value by which the pedestal was discriminated, and was obtained to be 10 %. N_{pe} at 4.0 GeV/c was calculated to be 2.74 ± 0.08 as listed in Table 2. This value is about 60 % smaller

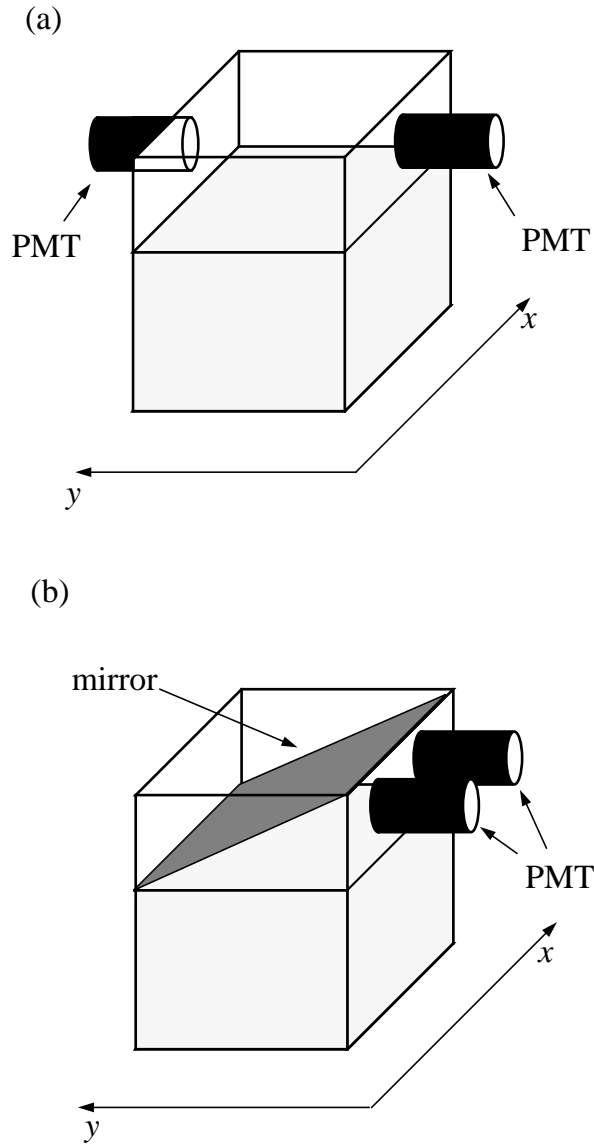


Fig.10

Figure 10: Schematic drawing of the test counter for tests of the light collection systems. The x - and y -directions are defined in the figure. The center of the counter was taken as the origin($(x, y) = (0, 0)$). (a) The diffuse scattering system. Two PMT's are faced each other(type A). (b) The mirror scattering system(type B). The mirror is made of thin aluminum, of which the surface is covered with MgF_2 .

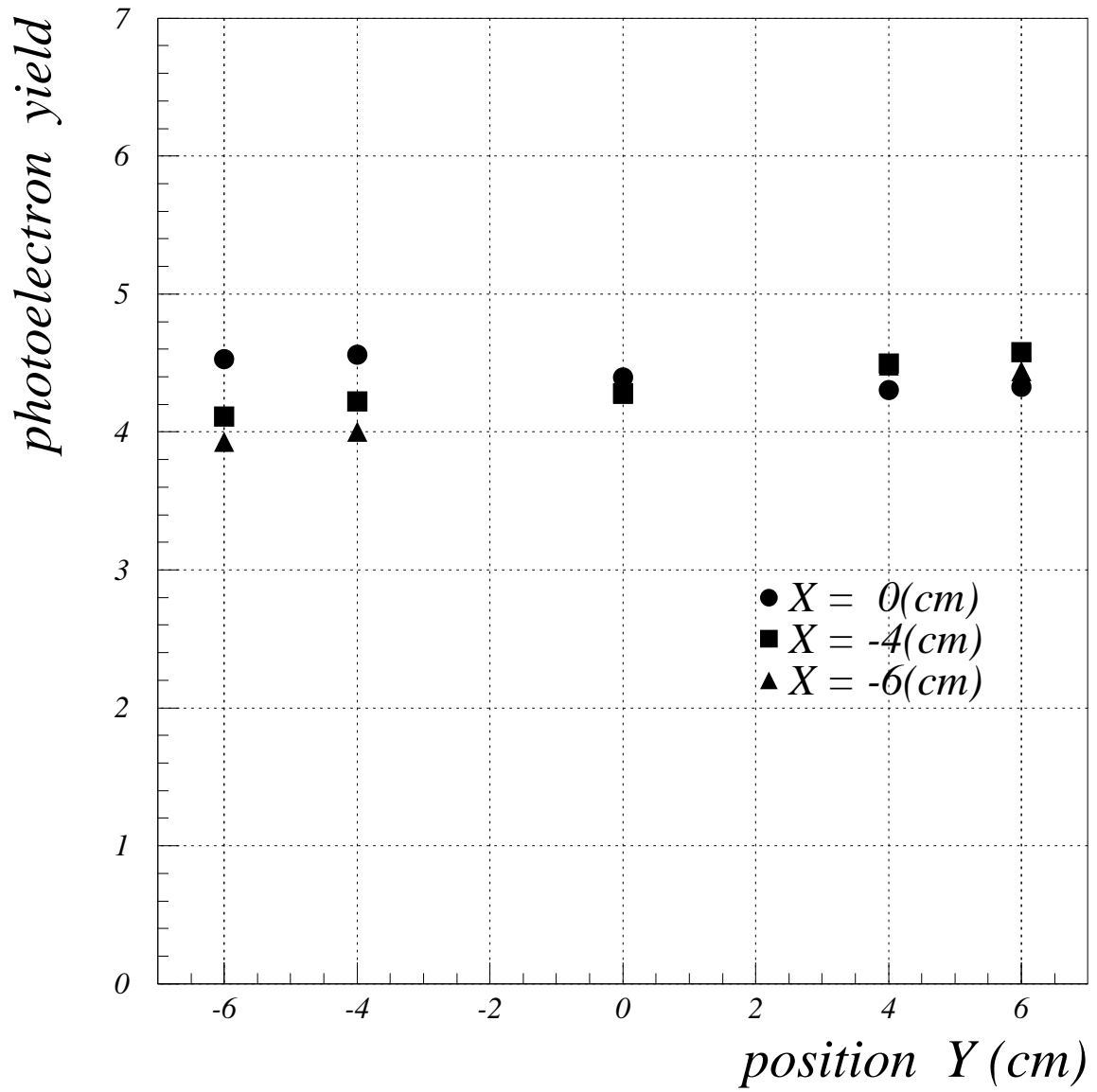


Figure 11: Average number of photoelectrons as a function of y (cm) at different x (cm) for a reference configuration. 4.0 GeV/c π was used.

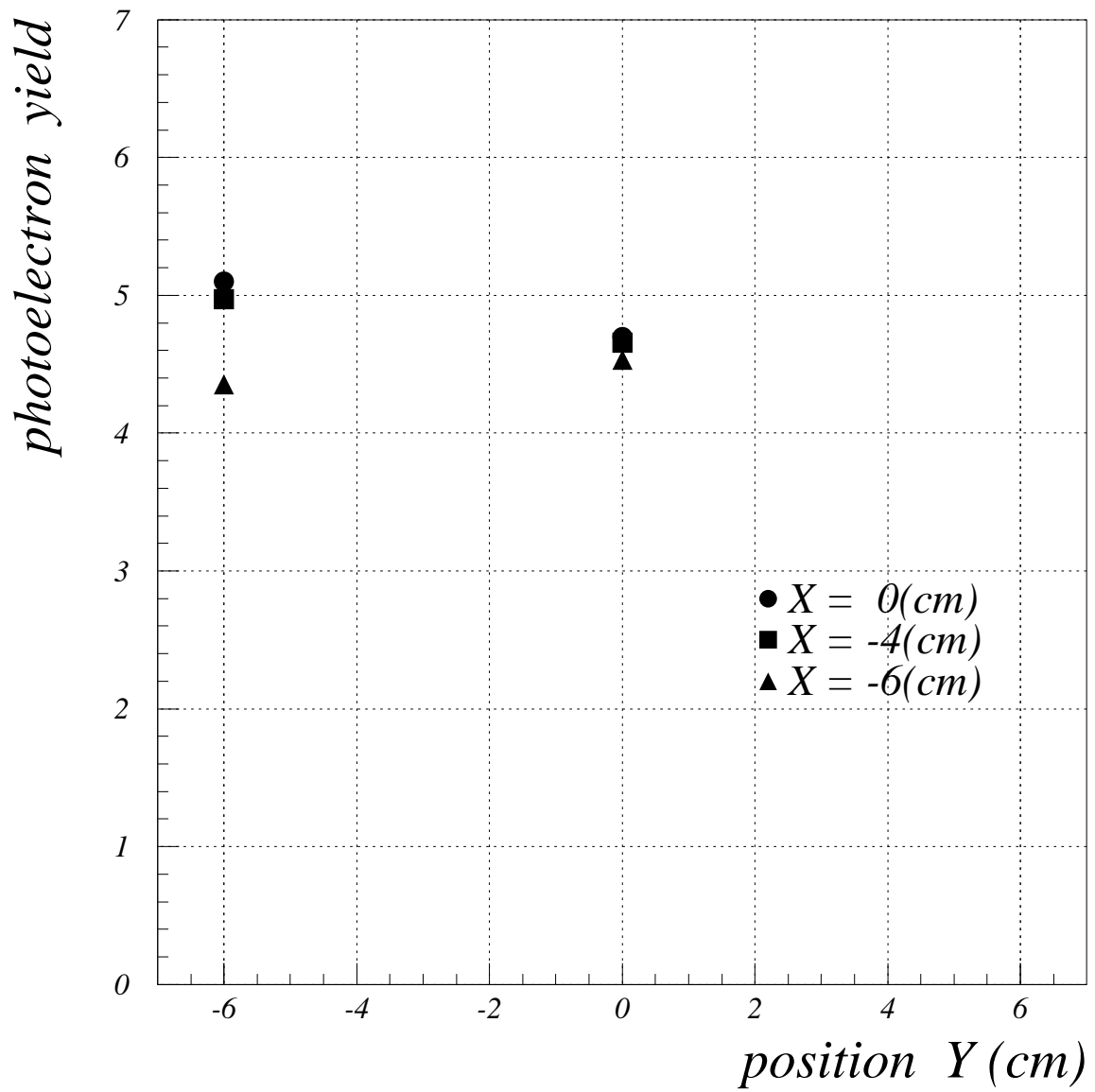


Figure 12: Same distribution of Fig.11, but for type A.

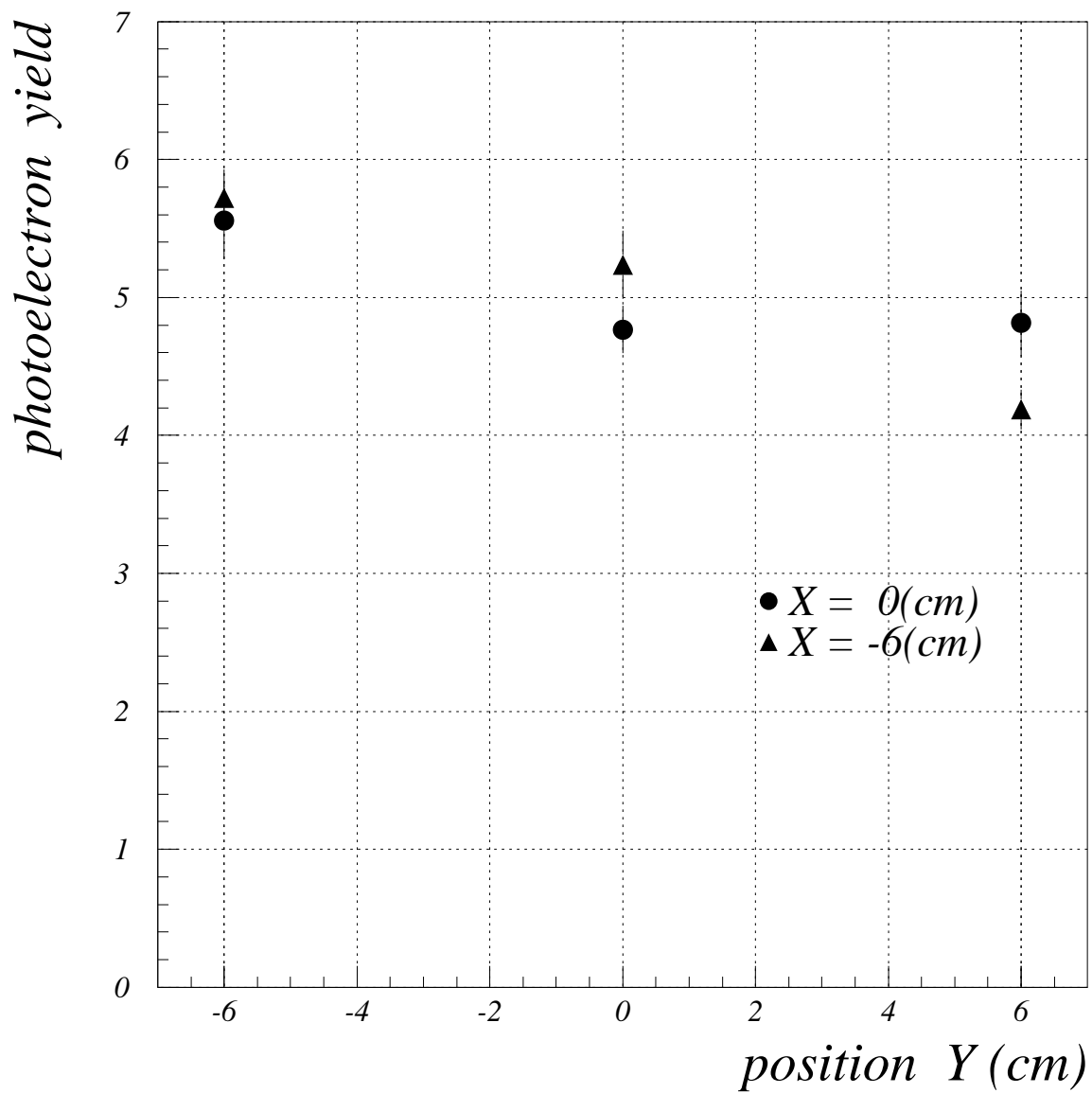


Figure 13: Same distribution of Fig.11, but for type B.

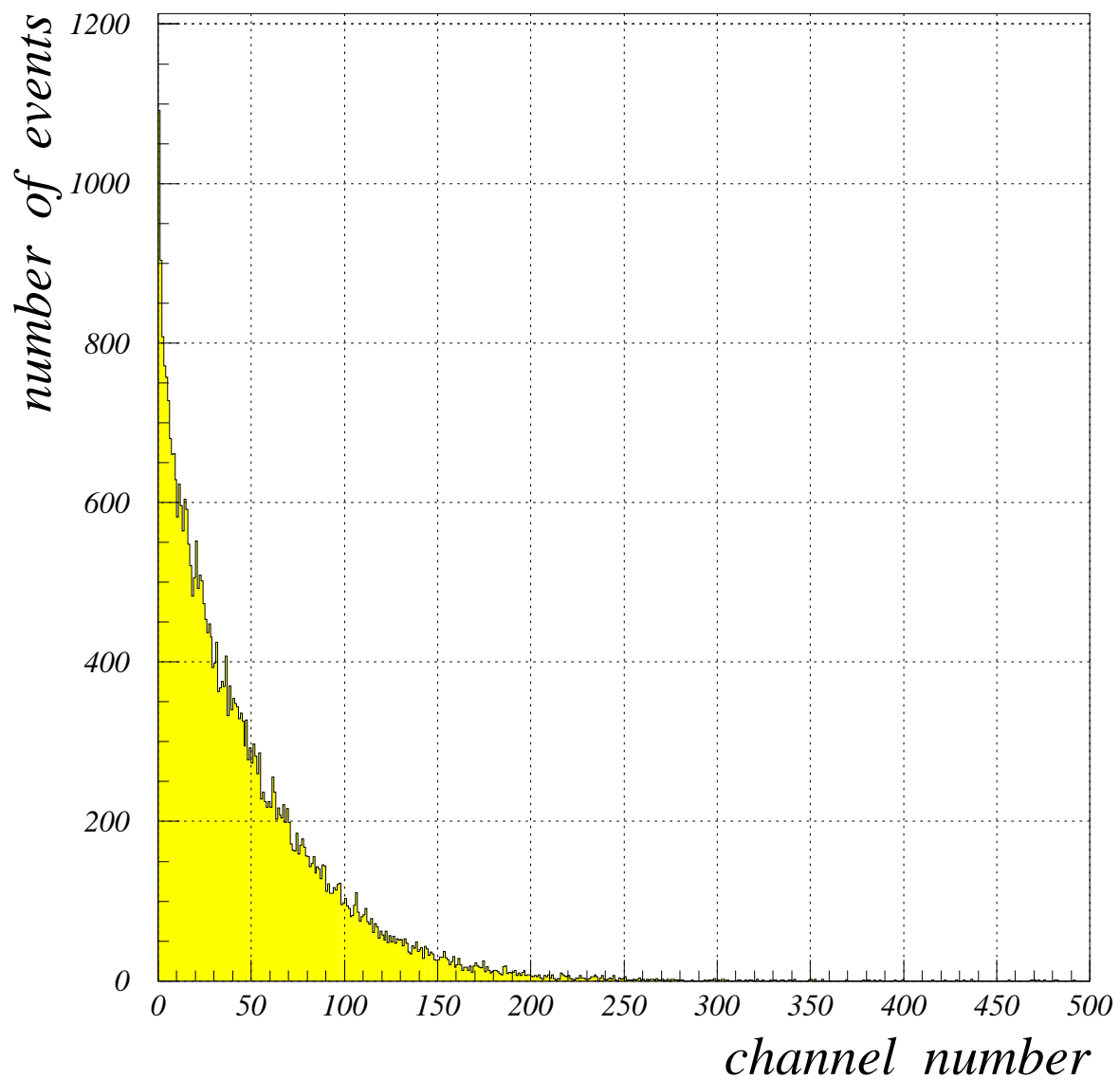


Figure 14: Pulse height distribution from one 2'' fine-mesh PMT at 4.0 GeV/c π .

than that from quantacon-type PMT's. The difference is considered to result from the sensitive area of a photocathode mounted in fine-mesh PMT's.

5 Detector Consideration

Based on these tests, we found that our aerogel has good characteristics. Light collection of type A(described in section 4) will be optimal since it gives reasonable number of photoelectrons and small position dependence.

The use of fine-mesh PMT's for the counter read out decreases the photoelectron yields. Nevertheless, the number of photoelectrons obtained from two 2'' fine-mesh PMT's (2.74 ± 0.08) is sufficiently large for a negative identification of K^\pm , However, it does not work as a positive identification of K^\pm out of a huge number of π^\pm . In the case of $B^\pm \rightarrow D^0 K^\pm$, for example, this feature is crucial[1].

According to these considerations, an increase in the photoelectron yields is particularly necessary. It can be improved by; (i) changing the refractive index from 1.013 to 1.018. By making this change, we can gain intrinsic Cherenkov photons by a factor of 1.4. Simultaneously, however, this trades the particle separation capability. The threshold momentum for K is reduced to be 2.59 GeV/c from 3.05 GeV/c. (ii) producing more transparent aerogels by optimizing some conditions in the production processes such as temperature. More transparent aerogels can increase the effective absorption length of the counter. This allows us to stack more aerogel sheets in the counter box.

Moreover, there are still some cracks in our aerogel as described in section 2. Thus, the optimizations of some parameters such as pressure in the supercritical drying should be done.

6 Conclusion

Silica aerogels having refractive indices of 1.013 have been successfully produced. A Cherenkov counter based on new aerogels was constructed, and its properties were studied with the test beam. The optical properties of aerogels were good enough to compensate for the intrinsically small number of photoelectrons emitted by a charged particle.

Two types of light collection systems, diffuse and mirror reflection, were tested. The mirror option provided a large number of photoelectrons, however, strong position dependence of the injection point was observed. The diffuse scattering option, on the other hand, gave reasonable results.

Moreover, fine-mesh photomultipliers, which are able to detect photons under a strong magnetic field, were used for the read out. The resultant light yields were marginally feasible for our experiment.

Based on these studies, our design of a Cherenkov counter, which can identify π and K in the region of $1.0 \sim 2.5$ GeV/c, was considered. To increase the number of photoelectrons observed with fine-mesh photomultipliers, the refractive index of silica aerogels should be increased to be $n = 1.018$.

Acknowledgement

This work was partially supported by a collaborative research program between Matsushita Electric Works, Ltd. and KEK. We are indebted to S. Iwata, F. Takasaki and M. Kobayashi at KEK for their continuous encouragement. We are grateful to H. Koike and S. Hirao at Matsushita Electric Works, Ltd. for their support. We thank all of the staff in Central Research Laboratory at Matsushita Electric Works, Ltd. We thank the KEK machine shop members for their help in constructing the test counter. H. Kawai is also acknowledged for stimulating discussions.

References

- [1] *B* Physics Task Force Group, Progress Report on Physics and Detector at KEK Asymmetric *B*-Factory, KEK Report 92-3, March, 1992; 1992 Progress Report on *B* Physics Task Force Activities, KEK Report 93-1, April.
- [2] Proceedings of Workshop on Physics and Detector Issues for a High-Luminosity Asymmetric *B* Factory at SLAC, SLAC Report-373, 1990.
- [3] P. Carlson, Nucl. Instr. and Methods **A248**(1986)110 and reference therein.
- [4] G. Poelz and R. Reithmüller, Nucl. Instr. and Methods **195**(1982)491.
- [5] S. Yasumi et al., KEK Report 83-25, March, 1983.
- [6] H. Kawai et al., Nucl. Instr. and Methods **228**(1985)314.
- [7] S. Toyama et al., INS-T-480, April, 1988.
- [8] L.W. Hrubesh, T.M. Tillotson and J.F. Poco, UCRL-Ext.Abs. 102518 preprint, LLL, 1990.
- [9] Matsushita Electric Works, Ltd., Japanese Patent Early Publication (KOKAI)No.1992-198238.
- [10] Hitachi Co. Ltd. model U-3210.
- [11] R. Enomoto et al., Nucl. Instr. and Methods **A332**(1993)129.